

## Magnetoresistance of Chromium Dioxide Powder Compacts

J. M. D. Coey,\* A. E. Berkowitz, Ll. Balcells,† and F. F. Putris

Center for Magnetic Recording Research, University of California, San Diego, La Jolla, California 92093

A. Barry

Physics Department, Trinity College, Dublin 2, Ireland

(Received 9 September 1997)

Cold-pressed powders of the half-metallic ferromagnet  $\text{CrO}_2$  are dielectric granular metals. Hysteretic magnetoresistance with maxima at the coercive field arises from interparticle contacts. Dilution with insulating antiferromagnetic  $\text{Cr}_2\text{O}_3$  powder reduces the conductivity by 3 orders of magnitude, but enhances the magnetoresistance ratio which reaches 50% at 5K. The negative magnetoresistance is due to tunneling between contiguous ferromagnetic particles along a critical path with a spin-dependent Coulomb gap. [S0031-9007(98)05996-1]

PACS numbers: 72.15.Gd, 73.40.Gk, 75.50.Cc, 81.20.Ev

Negative magnetoresistance has been widely investigated in ferromagnetic metals and heterostructures. Effects intrinsic to a material are distinguished from extrinsic effects which depend on the direction of magnetization in adjacent ferromagnetic regions. Examples of the former include the anisotropic magnetoresistance of permalloy [1] or the colossal magnetoresistance of nonstoichiometric  $\text{EuO}$  [2] and mixed-valence manganites [3]. Examples of the latter are the giant magnetoresistance of multilayers [4] and granular metals [5,6] or the behavior of spin-dependent tunnel junctions [7], where resistivity is greatest at the coercive or switching field and decreases as the sample reaches technical saturation. Recent experiments on epitaxial manganite films with a single grain boundary have allowed the high-field, colossal magnetoresistance to be separated from the low-field effect due to heterogeneous magnetization distribution in adjacent grains [8,9]. A characteristic but unexplained feature of the low-field magnetoresistance in manganite ceramics [10], polycrystalline films [11,12], and tunnel junctions [13,14] is its rapid decay with increasing temperature.

Here we report a new type of extrinsic magnetoresistance. It is studied in pressed powders of  $\text{CrO}_2$ , where it arises from contacts between particles. Chromium dioxide is an ideal material for spin-polarized electron tunneling, as it is a half-metallic ferromagnet where complete spin polarization of the conduction electrons is maintained up to the surface [15]. There are two  $3d$  electrons in spin-split  $t_{2g}$  subbands, one localized and the other in a half-filled band [16]. The two electrons are strongly coupled by the on-site exchange interaction  $J_H \approx 1$  eV. The intrinsic metallic nature of the oxide is illustrated by the resistivity of an oriented film grown on  $\text{TiO}_2$ , shown in Fig. 1(a). It follows Matthiessen's rule with a residual resistivity of  $0.1 \mu\Omega \text{ m}$  ( $10 \mu\Omega \text{ cm}$ ) and a room-temperature value about 30 times greater. The slope  $d\rho/dT$  remains positive above the Curie temperature ( $T_C = 396$  K) [17]. The films exhibit only a small linear intrinsic magne-

toresistance effect,  $(1/\mu_0\rho)d\rho/dH = \sim 1\%/T$  at room temperature.

Our samples were made from a commercial  $\text{CrO}_2$  powder used for magnetic recording. The powder is composed of acicular single-domain particles with an average length of 300 nm and an aspect ratio of about 8:1. Coercivity is 59 mT (590 G) at room temperature, rising up to 99 mT at 5 K. Disks with a diameter of 9 mm and thickness of  $\approx 0.8$  mm were cold pressed at 0.4 GPa. Typical densities are 45%, but values of up to 57% were achieved by additional compaction. No preferred orientation of the elongated particles was evident in scanning electron micrographs. Besides the single-component samples, we also prepared a series of composites where a weight fraction  $x$  of the  $\text{CrO}_2$  powder was mixed with a fraction  $(1-x)$  of antiferromagnetic insulating  $\text{Cr}_2\text{O}_3$  powder of the same particle size, prepared by reducing the  $\text{CrO}_2$  under vacuum at  $500^\circ\text{C}$ .

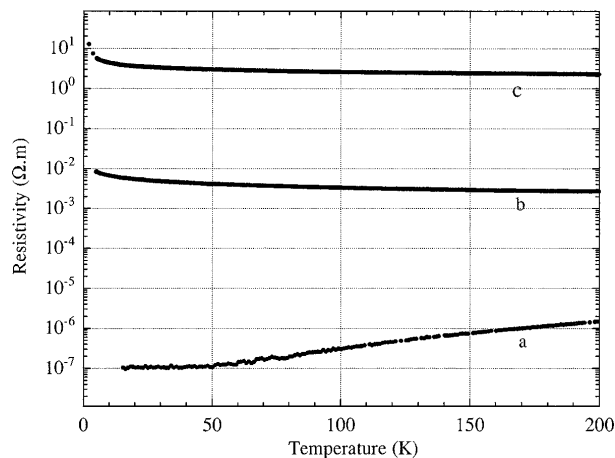


FIG. 1. Temperature dependence of the resistivity of (a) an epitaxial  $\text{CrO}_2$  film, (b) cold-pressed  $\text{CrO}_2$  powder, (c) a cold-pressed composite of 25% $\text{CrO}_2$  and 75% $\text{Cr}_2\text{O}_3$ .

Electrical resistance was measured by a 4-electrode method. Data for a  $\text{CrO}_2$  compact shown in Fig. 1(b) are typical of a granular metal [18]. The thousandfold increase over the intrinsic resistivity is attributed to the resistance of the interparticle contacts. From the particles' dimensions, the average interparticle contact resistance  $\langle R_{ij} \rangle$  is estimated as  $\approx 60 \text{ k}\Omega$ , considerably greater than the quantum limit  $R_Q = h/2e^2$ . Nevertheless, a very broad distribution of contact resistance is to be expected. Conduction through such an array of metallic particles with a random distribution of  $R_{ij}$  will be along percolation paths encompassing the lowest resistance contacts. These critical paths include weak conductance links where a single contact connects two larger clusters [19]. The  $\text{CrO}_2$  particles are sufficiently small and the contact resistance is sufficiently high for single-particle charging to influence the conductivity. The charging energy  $E_c \approx e^2/2C$  [18] where  $C$ , the capacitance of a particle, is  $4\pi\epsilon_0\epsilon r_{\text{av}}$ . Taking  $r_{\text{av}} = 125 \text{ nm}$  and an effective dielectric constant  $\epsilon = 5$  gives a charging energy of  $1.2 \text{ meV}$  ( $13 \text{ K}$ ).

The magnetoresistance of the  $\text{CrO}_2$  powder compact is shown in Fig. 2. Magnetization and resistance were measured simultaneously in fields up to  $5.5 \text{ T}$  in a SQUID magnetometer. There is a "butterfly" curve, with a reversible high-field slope. The zero field resistance  $R_0$  is defined by extrapolating this linear portion to zero field, and the magnetoresistance ratio  $\Delta R/R_0$  is defined as  $(R_{\text{max}} - R_0)/R_0$ . This type of hysteretic magnetoresistance is associated with alignment of the magnetization of the  $\text{CrO}_2$  particles since the maximum resistance practically coincides with the coercivity. The magnetoresistance ratio is  $29\%$  at  $5 \text{ K}$ , and it varies as  $\exp(-T/T_{\text{mr}})$ , where  $T_{\text{mr}} = 46 \text{ K}$  (Fig. 3). At room temperature  $\Delta R/R_0 < 0.1\%$ .

Results on the composites are even more remarkable. Fitting the resistivity of cold-pressed  $x\text{CrO}_2/(1-x)\text{Cr}_2\text{O}_3$  powders to the percolation theory expression [20]  $\rho = (x - x_p)^{-2}$  gives the percolation concentration

$x_p = 0.23$ . The dilute composites show much greater resistivity and greater magnetoresistance ratios. A sample with  $x = 0.25$  is very near the percolation threshold; its room-temperature resistivity is  $2 \Omega \text{ m}$ , a thousand times greater than for undiluted  $\text{CrO}_2$  powder, yet  $\Delta R/R_0$  at  $5 \text{ K}$  is  $50\%$ . The resistivity is shown in Fig. 1(c); with parameters  $\rho_\infty = 2.09 \Omega \text{ m}$  and  $\Delta = 6.0 \text{ K}$ , it can be fitted to the expression for granular metals in the dielectric regime [19].

$$\rho = \rho_\infty \exp(\Delta/T)^{1/2}, \quad (1)$$

where  $\Delta$  is proportional to  $E_c$ . The conductivity extrapolates to zero at  $T = 0$  (Fig. 5), and the magnetoresistance ratio extrapolates to  $56\%$  (Fig. 3).

The voltage dependence of the resistance can be measured in the dilute, high-resistance composites without any significant heating of the sample. The magnetoresistance ratio of  $25\%\text{CrO}_2/75\%\text{Cr}_2\text{O}_3$  at  $5 \text{ K}$  is halved when the potential drop across a sample reaches  $4 \text{ V}$  (Fig. 3). From the electrode separation ( $\approx 1 \text{ mm}$ ) it is estimated that there will be roughly  $10^4$  particles along a conduction path, but most of the voltage is expected to be dropped across some fraction, perhaps  $10\%$ , of these which have high-resistance contacts, giving an interparticle potential difference of a few mV. The number of particles involved is evaluated by comparing the voltage and temperature dependence of  $\Delta R/R_0$ . We assume that magnetoresistance at finite temperature is controlled by energy mismatch across the barriers or intermediate states that produce spin-flip scattering. In a broad distribution of particles, these both will be uniformly distributed in energy. Scaling the energy associated with temperature ( $k_B T$ ) and bias voltage across a single tunnel junction ( $eV_b$ ) then allows the temperature and voltage variation of  $\Delta R/R_0$  in Fig. 3 to be reconciled by setting  $4V \equiv 25 \text{ K}$ , which indicates that  $4e/25k_B \approx 1900$  of these contacts are involved in the

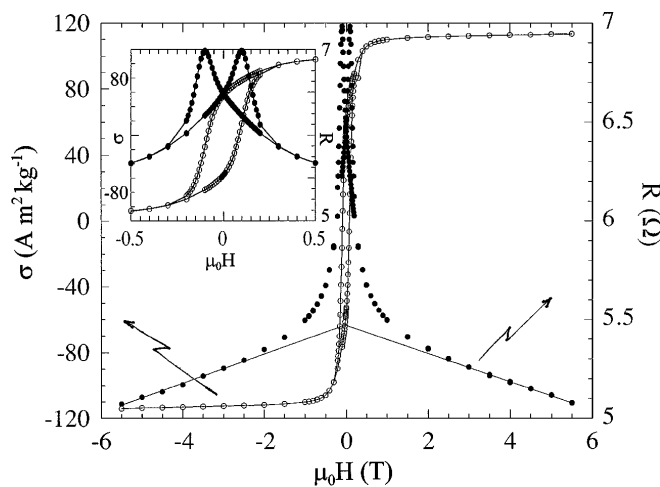


FIG. 2. Magnetization ( $\circ$ ) and resistance ( $\bullet$ ) of a  $\text{CrO}_2$  powder compact at  $5 \text{ K}$ . The inset shows detail at low field.

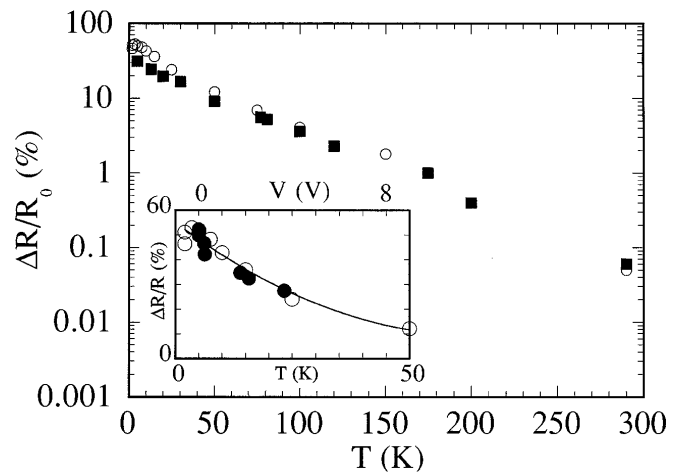


FIG. 3. Temperature dependence of the magnetoresistance ratio for  $\text{CrO}_2$  ( $\blacksquare$ ) and  $25\%\text{CrO}_2/75\%\text{Cr}_2\text{O}_3$  ( $\circ$ ) powder compacts. The inset compares the voltage ( $\bullet$ ) and temperature ( $\circ$ ) dependences for  $25\%\text{CrO}_2/75\%\text{Cr}_2\text{O}_3$ .

magnetotransport process. In a second sample with a shorter distance between electrodes, this procedure gives  $\approx 700$  contacts.

In order to appreciate how the high contact resistance of pressed powders leads to high magnetoresistance, we consider a weak conductance link in the percolation path (Fig. 4). Links in the critical path where a particle has only two neighbors and at least one relatively high-resistance contact are expected to contribute most to the measured resistivity. The current through a weak link is controlled by the relative orientation  $\theta_{ij}$  of the magnetization of the half-metallic particles. The resistance is

$$R = R_{12}/f(\theta_{12}) + R_{23}/f(\theta_{23}), \quad (2)$$

where  $R_{ij}$  depends on the barrier height, junction area, and thickness [21] and  $f(\theta_{ij})$  is the relative probability of electron transfer into the adjacent particle. Provided no spin depolarization occurs in the barrier,  $f(0) = 1$ , and the general expression is [22]

$$f(\theta) = \cos^2(\theta/2) + 2S/(2S + 1)^2 \sin^2(\theta/2), \quad (3)$$

which averages to  $\frac{1}{2}$  if the orientation of the particles' magnetization is random and the core spin  $S \gg 1$ . A 100% magnetoresistance ratio is predicted in that case. For  $\text{CrO}_2$ ,  $S = \frac{1}{2}$  which gives  $\langle f(\theta) \rangle = \frac{5}{8}$  for random orientations, hence the predicted  $\Delta R/R_0$  is 60%, in agreement with the zero-temperature value for the dilute sample (56%).

The drastic temperature dependence of the powder magnetoresistance (PMR) is comparable to that of the low-field magnetoresistance in manganite polycrystals [10] and heterostructures [13]. In our case, the similarity of the dependence on temperature and voltage suggests a connection with the Coulomb gap. In Fig. 5 we show  $I:V$  curves measured at 5 K at the resistance peak (0.1 T) and at ferromagnetic saturation (2 T), as well as the corresponding conductance, which doubles when the voltage per contact reaches about 1 meV. The voltage dependence of the conductance at 2 and 5 K is characteristic of a Coulomb gap, although the curves do not start at zero because the temperature is comparable to the gap energy. Furthermore, the data clearly indicate a larger gap in the misaligned, coercive state than in the aligned, saturated state. Helman and Abeles [23] first proposed an extra gap or mismatch energy  $E_m$  of magnetic origin to explain the magnetore-

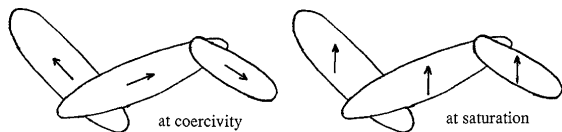


FIG. 4. A weak conduction link in a critical percolation path for conduction. Arrows indicate the directions of magnetization of the particles at the coercive field ( $\approx 0.1$  T) and at saturation (2 T).

sistance of granular nickel. Fitting the 5 K data to their expression for fully spin-polarized electrons

$$\sigma = \sigma_{\infty} \exp[-(E_c + E_m)/eV], \quad (4)$$

where  $E_m = 0$  in the saturated state gives  $E_c = 0.34$  mV (3.9 K), whereas in the coercive state  $E_c + E_m = 0.81$  mV. Hence  $E_m = 0.47$  mV (5.5 K). The 2 K data give  $E_c = 0.29$  mV and  $E_m = 0.31$  mV. The magnetic energy may be identified as the difference in exchange energy of contiguous, magnetically misaligned particles with  $n$  and  $n'$  electrons, and the same two particles with  $n - 1$  and  $n' + 1$  electrons; it is  $\approx J/2$ , where  $J$  is the interatomic exchange coupling mediated by the conduction electron. Both  $E_c$  and  $E_m$  are temperature dependent because tunneling at lower temperatures is "longer range" involving thicker (or higher) barriers but lower mismatches [23]. PMR depends on temperature partly because of the exchange contribution to the Coulomb gap. The temperature dependence of the conductivity in the disordered and saturated states is included in Fig. 5, together with the curves expected from Eq. (1) setting  $\Delta$  equal to the 5 K values of  $E_c$  and  $(E_c + E_m)$ . The apparent exponential variation of  $\Delta R/R_0$  is therefore a combination of this low-temperature behavior together with spin-flip scattering processes effective at higher temperature. Improved magnetoresistance ratios at higher

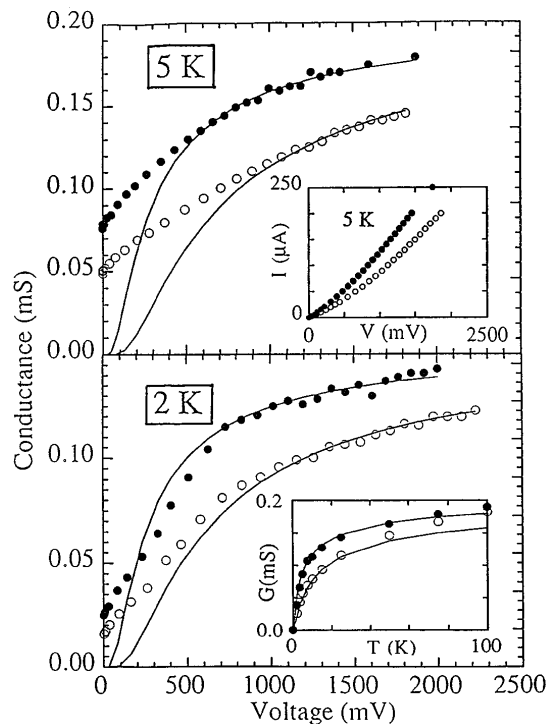


FIG. 5. Conductance at 5 and 2 K for the 25% $\text{CrO}_2$ /75% $\text{Cr}_2\text{O}_3$  composite measured in 0.1 T ( $\circ$ ) and in 2 T ( $\bullet$ ). The insets show  $I-V$  curves at 5 K from which the conductance is derived and the temperature dependence of the conductance, with solid lines given by Eq. (1). The number of resistive contacts in this sample is estimated to be 700.

temperature might be achieved by using larger particles to reduce  $E_c$ , and aligning the particles so that the magnetization of neighbors lie either parallel or antiparallel to enhance  $E_m$ .

Spin-flip processes are unlikely to involve phonons because even at room temperature most tunneling is expected to be elastic. A possible source of spin-flip scattering, specific to  $\text{CrO}_2$ , involves excitation of antiferromagnetic magnons in a surface layer of the thermodynamically stable oxide  $\text{Cr}_2\text{O}_3$ . The spin-wave gap of bulk  $\text{Cr}_2\text{O}_3$  is 8 K [24]. More generally, spin-flip scattering could also occur at weakly exchange coupled or misaligned  $\text{Cr}^{3+}$  ions at the  $\text{CrO}_2$  surface or in the interface. It is also possible that electrons tunnel into a magnetically misaligned particle with excitation of a surface [25] or bulk spin wave in the  $\text{CrO}_2$ . The energy required is of order  $T_C(a/w)^2$ , where  $a$  is the lattice parameter and  $w$  is the barrier thickness. It can contribute to  $E_m$ .

The reversible, linear high-field magnetoresistance (Fig. 2) is unrelated to coercivity. Its value  $(1/\mu_0 R_0)(dR/dH) \sim 1\%/T$  is also temperature and voltage dependent (Fig. 2), but it is only half as sensitive as  $\Delta R/R_0$  to changes in either. It falls as  $\exp(-T/T_{\text{hf}})$  with  $T_{\text{hf}} = 87$  K. Like the magnetoresistance, the voltage and temperature dependence can be reconciled by setting  $4 \text{ V} \equiv 25 \text{ K}$  in the first sample, but the physical processes occurring at the contacts must be different since the characteristic energy scales  $T_{\text{mr}}$  and  $T_{\text{hf}}$  differ by a factor of 2. The effect might be intrinsic to  $\text{CrO}_2$ , associated with the tiny change in chemical potential  $g\mu_B SB (= 0.12 \text{ mV/T})$  which results when a magnetic field is applied to a half-metallic ferromagnet. Other possibilities are that the applied field reduces the effective height or width of the tunnel barriers, e.g., by modifying the width of a layer of localized charge at the surface, or that it polarizes disordered spins in the interface.

In conclusion, this first study of magnetotransport in a granular half-metallic ferromagnet has revealed a large extrinsic magnetoresistance in pressed powder compacts of  $\text{CrO}_2$ . The powder magnetoresistance effect is associated with the magnetization process of particles in poor electrical contact with each other. The voltage and temperature dependence of  $\Delta R/R_0$  are related to a spin-dependent Coulomb gap. Spin polarization of the tunneling electrons in  $\text{CrO}_2$  is near complete below 5 K. We have observed similar effects in powder compacts of other materials with a high degree of spin polarization, such as magnetite and ferromagnetic manganites [26]. It will be possible to control the PMR by varying the particles' shape, size, orientation, and surface state. Our results also suggest that much greater magnetoresistance ratios will be found in aligned  $\text{CrO}_2$  powders or structured spin-dependent tunnel junctions made from this extraordinary black oxide.

The authors benefited from discussions with R.C. Dynes, F. Guinea, F. Hellman, Pang Xiong, and S. Sankar. They are grateful to E. Price and D. Schurig for experimental help. The work was partly supported by NSF Grant No. DMR 9400439, by CIRIT (Spain), and by the EC OXSEN-TMR network. The  $\text{CrO}_2$  powders were kindly supplied by J.H. Kidd, DuPont Films, Newport, DE.

\*Permanent address: Physics Department, Trinity College, Dublin 2, Ireland.

†Permanent address: ICMAB, Campus UAB, E-08019 Bellaterra, Spain.

- [1] T.R. McGuire and R.I. Potter, IEEE Trans. Magn. **11**, 1018 (1975).
- [2] T. Penney, M.W. Shafer, and J.B. Torrance, Phys. Rev. B **5**, 3669 (1972).
- [3] S. Jin *et al.*, Science **264**, 413 (1994).
- [4] M. Baibich *et al.*, Phys. Rev. Lett. **61**, 2472 (1988).
- [5] A.E. Berkowitz *et al.*, Phys. Rev. Lett. **68**, 3745 (1992).
- [6] J.Q. Xiao, J.S. Jiang, and C.L. Chien, Phys. Rev. Lett. **68**, 3749 (1992).
- [7] J.S. Moodera, L.R. Kindaer, T.M. Wong, and R. Meservey, Phys. Rev. Lett. **74**, 3273 (1995).
- [8] N. Mathur *et al.*, Nature (London) **387**, 266 (1997).
- [9] K. Steenbeck *et al.*, Appl. Phys. Lett. **71**, 968 (1997).
- [10] H.Y. Hwang, S.W. Cheong, N.P. Ong, and B. Batlogg, Phys. Rev. Lett. **77**, 2041 (1996).
- [11] R. Shreekala *et al.*, Appl. Phys. Lett. **71**, 282 (1997).
- [12] X.W. Li, A. Gupta, G. Xiao, and C.Q. Gong, Appl. Phys. Lett. **71**, 1124 (1997).
- [13] Y. Lu *et al.*, Phys. Rev. B **54**, R8357 (1996).
- [14] M. Viret *et al.*, Europhys. Lett. **39**, 545 (1997).
- [15] L.H.v. Leuken and R.A.d. Groot, Phys. Rev. B **51**, 7176 (1995).
- [16] M.A. Korotin, V.I. Anisimov, D.I. Khomskii, and G.A. Sawatzky (unpublished).
- [17] L. Ranno, A. Barry, and J.M.D. Coey, J. Appl. Phys. **81**, 5774 (1997).
- [18] B. Abeles, P. Sheng, M.D. Coutts, and Y. Arie, Adv. Phys. **24**, 407 (1975).
- [19] P. Sheng, Philos. Mag. B **65**, 357 (1992).
- [20] K. Stauffer, *Introduction to Percolation Theory* (Taylor and Francis, London, 1985).
- [21] R. Meservey and P.M. Tedrow, Phys. Rep. **238**, 173 (1994).
- [22] F. Guinea (unpublished).
- [23] J.S. Helman and B. Abeles, Phys. Rev. Lett. **37**, 1429 (1976).
- [24] E.J. Samuelsen, M.T. Hutchings, and G. Shirane, Physica (Utrecht) **48**, 13 (1970).
- [25] S. Zhang, P.M. Levy, A.C. Marley, and S.S.P. Parkin, Phys. Rev. Lett. **79**, 3744 (1997).
- [26] J.M.D. Coey, A.E. Berkowitz, Ll. Balcells, F.F. Putris, and F.T. Parker, Appl. Phys. Lett. **72**, 734 (1998); J.M.D. Coey, Philos. Trans. R. Soc. A (to be published).